

E12He RLC Resonant Circuits

Lab Group 11: Mirzokhid Ganiev (3763884), Calina Burciu(3770859)

1 Introduction

This experiment will be utilising RLC circuits to understand the effect of resistance and circuit configuration on the resonance frequency of constant capacitance and inductance of Conductor and a Inductor. RLC circuits are fundamental in building a signal filtering system, where depending on the configuration of the circuit, it creates a band of set frequencies which are either allowed or not allowed through. The resonance behaviour of these circuits, noted as the frequency range in which the impedance of the capacitor and the inductor are equal, are points of such band filtration. Identifying the resonance frequency will be finding some global extremum within our set of input frequency from a Oscilloscope Random Wave Generator function. This experiment aims to analyse and compare the frequency-dependent behavior of Series and Parallel RLC circuits, focusing on the characterization of resonance frequency, the Full Width at Half Maximum (FWHM), damping constant, and quality factor Q . Both theoretical derivations and experimental validations are employed to evaluate the above discussed effects on the circuit. The data analysis focuses on understanding resonance characteristics, with theoretical support from Thomson's equation and impedance-based derivations. A further objective is to assess how well the extracted parameters align with expected values, and to examine sources of deviation and uncertainty, including limitations in measurement and data fitting techniques. The investigation highlights the significance of proper component selection and measurement accuracy in achieving reliable circuit analysis, with applications extending into real-world analogue systems and filter design.

2 Theoretical Exploration

The two circuit set ups, namely the Parallel and Series RLC circuits, function as Band-Stop filter or a Band-Pass filter respectively. To understand the behavioural elements of these two set ups, for different values of damping resistance, R_d , the resonance frequency, the Full Width at Half Maximum (FWHM), the damping coefficient, δ , and the rate of power dissipation, Q factor will have to be analysed.

Resonance happens due to the oscillation of the energy between the two types of energies stored in the two components; Electric inside the Capacitor and Magnetic in the Inductor. As such f_0 always correlates to the point at which the impedance of the two energy-storing components is at its minimum. Which leads to Thompson Equation as follows, with X_L reactance of the Inductor and X_C reactance of the Capacitor, where the minimum impedance occurs when the reactance of both components are equal. With $X_L = 2\pi fL$ $X_C = \frac{1}{2\pi fC}$, and meeting the condition $X_L = X_C$, leads to the following;

$$f = \frac{1}{2\pi} \cdot \frac{1}{\sqrt{LC}} = f_0 \quad (1)$$

where Eq. 1 is the equation to approximate the resonant frequency when C and L are known or calculated, the capacitance and inductance of the respective component.

The FWHM value is defined as the width at a height half of the maximum power calculated for a said set-up. With the power generated being correlated as $P = \frac{U_R^2}{R_d}$ and $P_{\frac{1}{2}} = \frac{P_{max}}{2}$, the two points in a Power against Frequency graph that correlate to the width would be defined as;

$$(y_1, x_1) = (f_1, \frac{P_{max}}{2}) \quad (y_2, x_2) = (f_2, \frac{P_{max}}{2}) \quad (2)$$

leading to FWHM, Δf being;

$$\Delta f = (f_2 - f_1) \quad (3)$$

With Eq. 3, the damping coefficient, δ , and the Q-factor would be evaluated as;

$$\delta = \pi \cdot \Delta f \quad (4)$$

$$Q_f = 2\pi \cdot \frac{f_0}{(f_2 - f_1)} \quad (5)$$

where both Eqs. 4 and 5 will be the equations used for the series set ups. All of the equations above correlate to both set ups, and will be utilised as such.

The following equation (Ziese, M. Practical Physics) describes how fitting parameters, namely U_0 , δ and f_0 , can be related to the frequency-dependent voltage:

$$U_R = \frac{2\delta\omega U_0}{\sqrt{4\delta^2\omega^2 + (\omega^2 - \omega_0^2)^2}}. \quad (6)$$

while $\omega = 2\pi f$. Also, the damping constant depends on the resistor as followed:

$$\delta = \frac{R}{2L} \quad (7)$$

3 TASK I, II: Series Resonant Circuit

3.1 Hypothesis

As per the behaviour of AC circuits, a series connected RLC circuit will behave in the same manna as a band pass filter. Where only a set of frequencies within some frequency band will be let through. This would create a rising Gaussian-like graph with one central peak. The peak will have to correspond to the resonance frequency.

3.2 Experimental Exploration

3.2.1 Materials

- Inductor of 5000 VISATON

- Capacitor
- Resistors 10Ω and 100Ω
- Adapter BNC-female pin
- Breadboard
- Residual items: Jumper wires, Laptop, Cabels, Screwdriver 2.5 mm, etc...

3.2.2 Set Up

For the series set up of the RLC circuit, all the electric components (Resistor, Capacitor, and the Inductor) are connected in series, with Picoscope's Random Wave Generator as the power source and Frequency Generator. With the Oscilloscope measurement tool in parallel across the resistor.

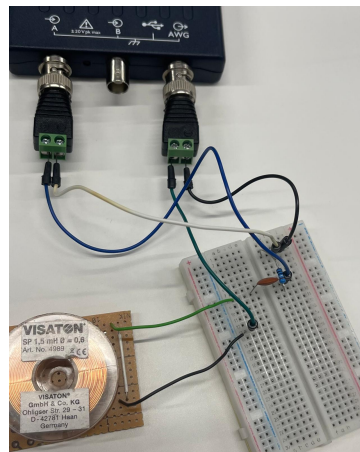


Fig 1 Set up for the Series Configuration.

3.2.3 Methodology

With the input voltage monitored and set at a set value (1V), the voltage drop across the resistor is measured with a varying input frequency. The measurement range is set up from 1 kHz up to 75 kHz, which includes the normalised voltage range, i.e $0.2 \leq \frac{U_R(f)}{U_R(f_0)} \leq 1$. With increments of 0.5 kHz from 1-10 (kHz) and then increments of 5 kHz from 10-75 (kHz). A total of 31 data points.

From the measured data, both voltage against frequency and current against frequency graphs would be presented. With resonance frequency identified as the global extremum within the set range.

3.3 Results

3.3.1 Data and Analysis

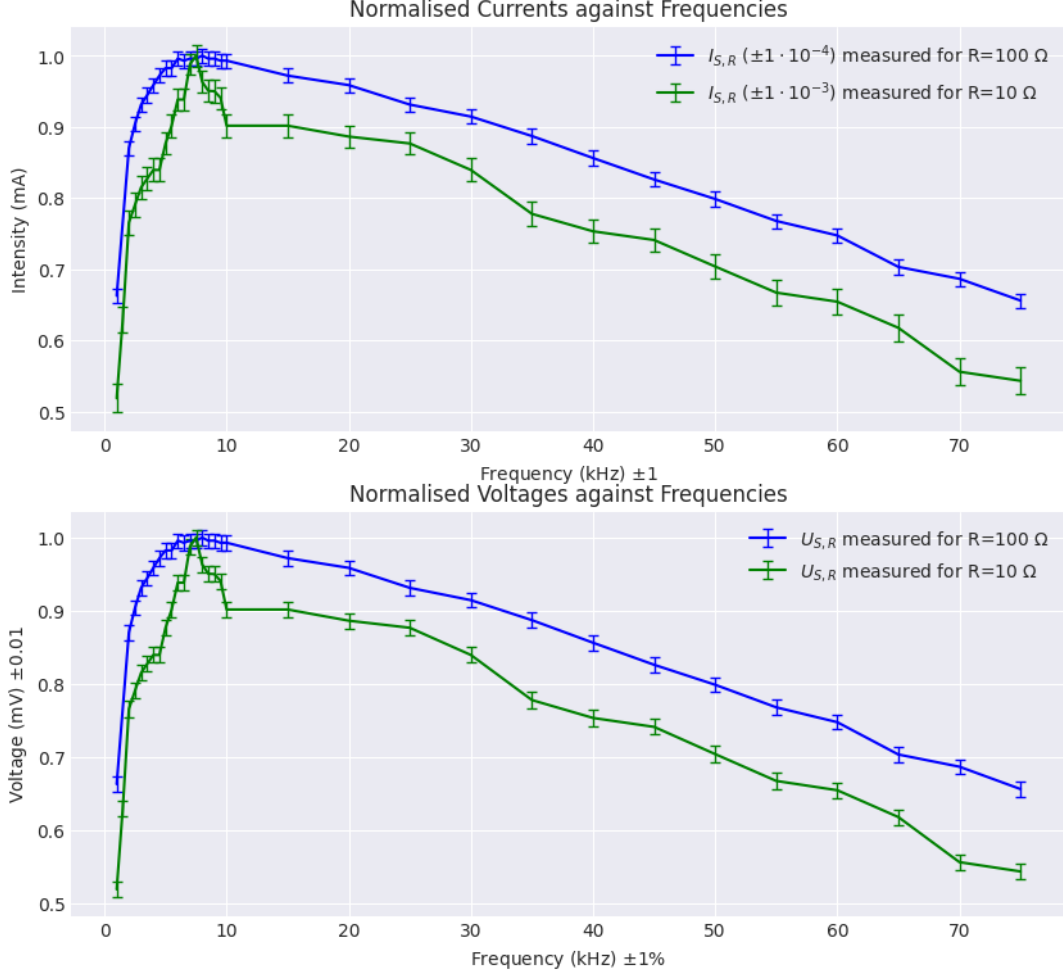


Figure 1: The Normalised Voltage and Current Frequency, $U_{S,R} \propto f_s$, $I_{S,R} \propto f_s$

Note: The uncertainties are as seen on the graph. For voltage, the measured uncertainty corresponded to the smallest measurable value. However as Current is derived from dividing the voltage by a constant known value of the respective resistance, the uncertainty for current is a constant multiple of the respective reciprocal of the resistor. Any further uncertainties, i.e not Current or Voltage, correspond to percentage uncertainties derived from the PicoScope Manual, or other reliable sources.(PicoScope)(Calculator.net. Resistor Calculator)

The resonance frequency of the circuit with the resistor of $100 \pm 3 \Omega$ is observed at 7.5 ± 0.07 kHz with a voltage of 141.9 ± 0.01 mV. For the resistor of $10 \pm 0.3 \Omega$, the resonance frequency is also observed at 7.5 ± 0.07 kHz, with voltage of 119.61 ± 0.1 mV.

All collected data points satisfy the normalized intensity range condition ($0.2 \leq \frac{I_R(f)}{I_R(f_0)} \leq 1$), so no points were excluded from the analysis. This confirms that the entire dataset is within the range of interest.

The parameter values obtained from the Full Width at Half Maximum (FWHM) method include the damping constants δ and the quality factors Q . For the first resistor, the fitted parameters are obtained: $\Delta f_{s1} = 58.00 \text{ kHz}$, $\delta_{s1} = 182.21 \text{ kHz}$ and quality factor $Q_{s1} = 0.04$. For the resistor of $10 \pm 0.3 \Omega$, the quality factor is $Q_{s2} = 0.06$, $\Delta f_{s2} = 43.00 \text{ kHz}$, $\delta_{s2} = 135.09 \text{ kHz}$.

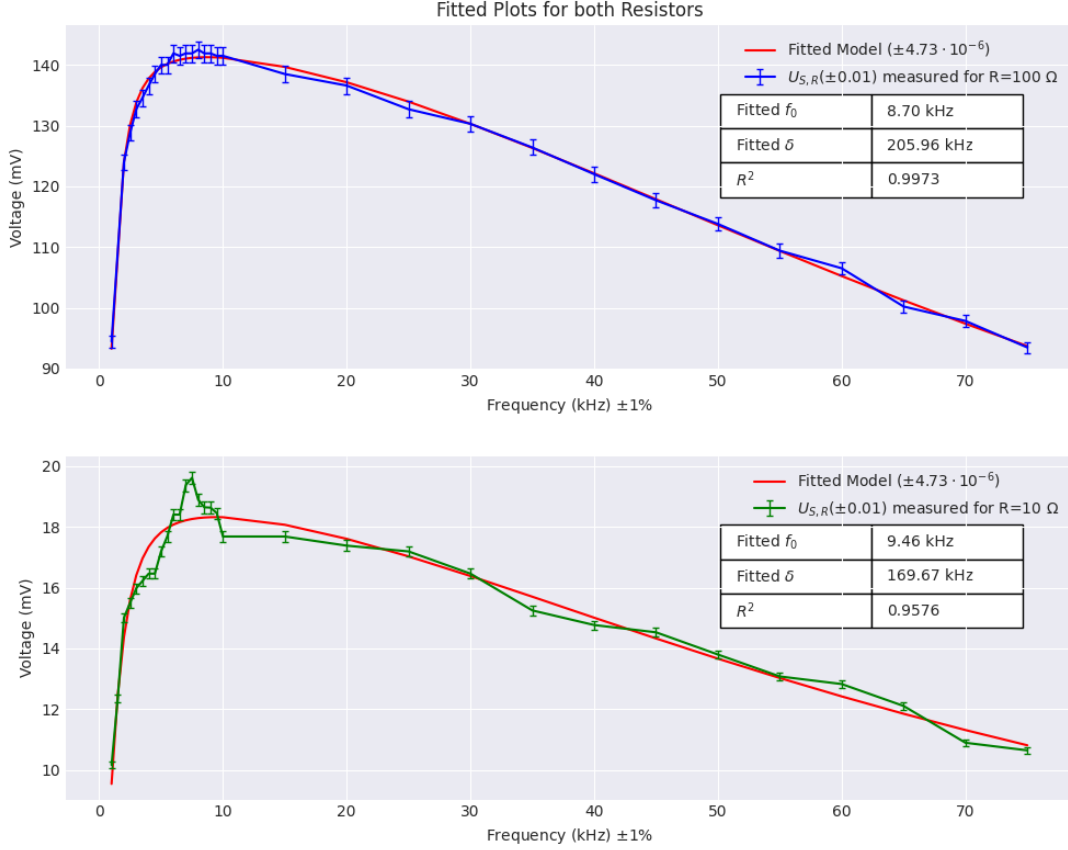


Figure 2: Fitted Curves for the Normalised Voltage and Current Frequency, $U_{S,R} \propto f_s$, $I_{S,R} \propto f_s$

In the second part of Task II, a fitted curve is done using the model described in Eq.6, and the capacitance is determined using Eq.1.

For the first resistor ($100 \pm 3 \Omega$), the fitted parameters are $f_{0s1} = 8.70 \text{ kHz}$ and $\delta_{s1} = 205.95 \text{ kHz}$, with a $R_{s1}^2 = 0.9972$. For the second resistor ($10 \pm 0.3 \Omega$), the fitted parameters are $f_{0s2} = 9.46 \text{ kHz}$ and $\delta_{s2} = 169.66 \text{ kHz}$, with $R_{s2}^2 = 0.9576$. In theory, as predicted by the Thomson equation, the found resonance frequency has to be the same regardless of the resistor being applied. As f_{os} is dependent only on the capacitance and inductance. However, clearly seen here, f_{os} differs, even if within the same magnitude. Possible explanation for such disparity will be discussed in the discussion.

Capacitance was determined using the resonance frequency and the Thomson resonance condition. For the first resistor, the capacitance is calculated to be 1.36 mF with an inductance of 0.24 H , while for the second resistor, the capacitance is 9.27 mF with an inductance of 0.04 H . Similarly, as for f_{os} , such differences (where it has to have stayed the same as there was no changing of components except the resistor) will be explored further in discussion.

3.3.2 Discussion

The graphs represent the resonance curves of the two resistors, as shown in Fig. ???. The resonance frequency is found by identifying the peak of the measured voltage.

In a series RLC circuit, the resonance curve is expected to be a smooth, monotonic function with a global extremum, where the resistor value affects the sharpness of the resonance peak. As expected, the data reflect this theoretical behavior. The smaller resistor produces a sharper and more chaotic peak, due to the lower damping and increased sensitivity to noise and fluctuations. In contrast, a larger resistor results in a smoother peak and more stable values around the resonance frequency. The resonance frequency is expected to remain approximately the same regardless of the resistor used, since it depends only on the inductance and capacitance of the circuit, not on the resistance (Eq. 1).

The FWHM method, as discussed in the theoretical exploration, is used to determine the damping constant δ and the quality factor Q . The code searches for points where the power equals half the maximum power. If no exact value exists in the dataset, it selects the nearest higher neighbour. Once the half-power frequencies are identified, Δf (the width at half maximum) is calculated, and from this, the damping constant is computed with Eq. 1. This method isn't preferred over curve fitting.

Although curve fitting can smooth or distort measured data, particularly in regions with sparse sampling, a high R^2 value suggests it still captures the overall trends of frequency-dependent voltages well. However, in cases like the second resistor, where the curve fitting fails to accurately model the maximum voltage, the FWHM method proves reliable, as FWHM is a geometric measurement from the plotted frequency response. FWHM is less affected by smoothing or distortion, making it more efficient for analyzing sharp peaks or noisy data around the resonance frequency. While both methods are valid, curve fitting is more effective for larger resistances, where the resonance curve is broader, and FWHM is better suited for smaller resistances with sharper peaks, as it provides a more direct measurement of the resonance characteristics.

The resonance frequency varies between the two resistor values, with a difference of approximately 0.76 kHz. This corresponds to a relative error margin of 8.73%. Despite the limitations and inconsistencies present in the experimental data, this level of agreement is considered reasonably acceptable for practical applications.

The model parameters that result from the fit represent the best match to your actual data when R^2 is sufficiently large, like in our case $R_{s1}^2 = 0.9972$ and $r_{s2}^2 = 0.9576$, while methods like FWHM only focus on a narrow portion of the resonance peak, which can lead to approximations.

In an ideal case, the capacitance and inductance should be independent of the resistors connected in the circuit. However, our measurements show a consistent difference in the extracted values. For the smaller resistor, the fitted capacitance is $C_{s1} = 1.37mF$, whereas for the larger resistor, it increases to $C_{s2} = 11.16mF$. Although it appears that the capacitance is changing, the physical capacitor itself remains the same. This apparent change arises from indirect measurement methods: the impedance seen by the capacitor depends on the surrounding circuit, particularly the resistors. When fitting a model to the measured voltage or current behavior, the extracted capacitance can vary, not because the capacitor changes, but because the model adapts to the overall impedance profile.

In essence, the capacitor is not changing; rather, its behavior within the specific circuit context is different. The same reasoning applies to the inductor.

The difference in f_{os} is largely due to how the Thompson equation ignores the effects of the resistor. Such an estimation of the oscillatory system is valid for small enough resistances but in deriving a more general formula, the f_{os} comes out to (Wikipedia contributors. RLC Circuit - Series RLC Circuit);

$$f_{os} = \sqrt{\frac{1}{LC} - \frac{R^2}{4L^2}} \quad (8)$$

The above equation presents a more accurate representation, and as such shows how the difference in resistance does effect the found value - even if a small difference.

Further improvements for this experiment will be measuring the effects at a much larger resistance, and understanding to what extent the resistance is negligible for the Thompson equation to hold.

3.3.3 Error Analysis

The uncertainty, as also seen on each graph for respective uncertainty, for the measured voltage data set is the smallest measurable value on the provided software. While the uncertainty for the Model Curve Fit Data Set is calculated following the equations of John R. Taylor, from An Introduction to Error Analysis: The Study of Uncertainties in Physical Measurements (Taylor):

$$\sigma_{U_R} = \left| \frac{\partial U_R}{\partial \omega} \right| \cdot \sigma_{\omega} \quad (9)$$

where utilising the above equation gives,

$$\sigma_{U_R} = \left| \frac{2\delta U_0 \left[\sqrt{4\delta^2 \omega^2 + (\omega^2 - \omega_0^2)^2} - \frac{(4\delta^2 \omega + 2\omega(\omega^2 - \omega_0^2)) \cdot \omega}{\sqrt{4\delta^2 \omega^2 + (\omega^2 - \omega_0^2)^2}} \right]}{(4\delta^2 \omega^2 + (\omega^2 - \omega_0^2)^2)} \right| \cdot \sigma_{\omega} \quad (10)$$

and when propagating the uncertainty through equation 10, leads to the summary of the uncertainties for the series circuit as:

Data Set	Mean Error Propagation	Largest Error (Max)
Model Curve Fit Voltage	$\pm 4.73 \cdot 10^{-6}$	$\pm 5.42 \cdot 10^{-5}$
Measured Voltage	± 0.01	± 0.01

Table 1: Error Propagation; Mean and Maximum Values

4 TASK III, IV: Parallel resonant circuit

4.1 Hypothesis

As parallel circuits present a band-stop filtering system, where all frequencies except the frequencies inside the band, are let through. Such a circuit will show a dip rather than

a rising maximum. However, in the same sense as for a band-pass filter seen in series, the frequency for the global extremum would corresponds to the resonance frequency.

4.2 Theoretical Exploration

In deriving the Voltage Output measured at the resistor for a Parallel Circuit, the method of a voltage divider will be utilised;

$$U_{P,R} = \frac{U_0 R}{|Z|} \quad (11)$$

where Z is the impedance of the circuit, which is derived from the following (where the resistor is connected in series to a parallel connected inductor and capacitor);

$$Z = R + \frac{1}{\frac{1}{X_L} + \frac{1}{X_C}} \quad (12)$$

With $X_L = j \cdot (\omega L + R_{sd})$, $X_C = \frac{1}{j\omega C}$, and R_{sd} being the internal resistance of the inductor coil. ω being the angular frequency, relating to the input frequency as $\omega = 2\pi f_p$. Plugging in and rearranging leads to;

$$Z = R + \frac{\frac{1}{\omega C j} j(\omega L + R_{sd})}{j(\omega L + R_{sd}) + \frac{1}{\omega C j}} \quad (13)$$

, where with further simplifications, the final equation for the impedance yields to;

$$Z = R + j \frac{\omega L + R_{sd}}{1 - \omega^2 LC - \omega R_{sd}} \quad (14)$$

where equation 14, when plugged into equation 11 from above, where the magnitude is defined as the square root of the squares of the real and imaginary part of the impedance, the final equation comes out to;

$$U_{P,R} = \frac{U_0 \cdot R}{\sqrt{R^2 + (\frac{\omega L + R_{sd}}{1 - \omega^2 LC - \omega R_{sd}})^2}} \quad (15)$$

Equation 15 is further supported by equating $X_L = j \cdot (\omega L + R_{sd})$ and $X_C = \frac{1}{j\omega C}$, and rearranging to get $\omega^2 LC + \omega R_{sd} C = 1$, which cancels out with 1 in the denominator of equation 14, making it an 'ignorable' term. Equation 15 will be utilised in producing a curve fit model for the measured data and finding R, R_{sd}, L, C parameters.

4.3 Experimental Exploration

4.3.1 Materials

- Inductor of 5000 VISATON
- Capacitor
- Resistor 100Ω
- Adapter BNC-female pin

- Breadboard
- Residual items: Jumper wires, Laptop, Cabels, Screwdriver 2.5 mm, etc...

4.3.2 Set Up

For the Parallel set up of the RLC circuit, the Inductor and the Capacitor are connected in parallel. With those components in series with the Resistor. The Peciscope's Random Wave Generator is connected as the power source and the frequency producer, and the Peciscope's measurement tool in parallel across the resistor.

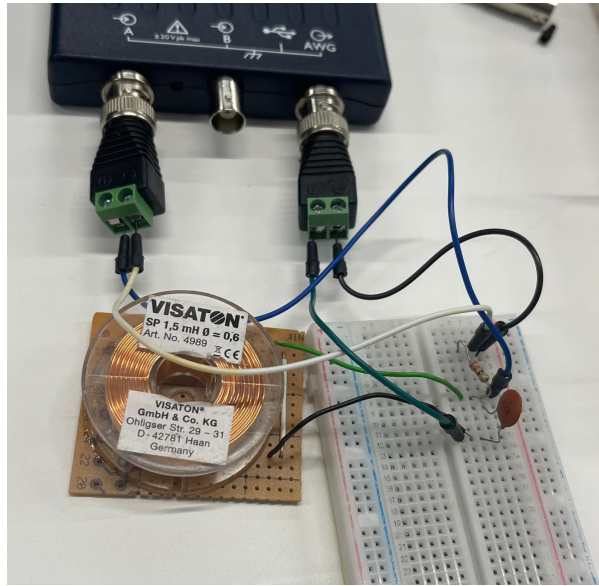


Fig 2 Set up for the Parallel Configuration.

4.3.3 Methodology

With the input voltage monitored and set at a constant value of 1V, the voltage drop across the resistor is measured with a varying input frequency. The measurement range is set up from 1.5 kHz up to 17 kHz, which includes the normalised voltage range, i.e $0.2 \leq \frac{U_{P,R}(f)}{U_{P,R}(f_0)} \leq 1$. With increments of 0.5 kHz from 1.5-8.5 (kHz) and 11-17 (kHz). Increments of 0.3 kHz from 8.5-9 (kHz) and 0.1 increments from 9-11 (kHz). A total of 41 data points. The inconsistent increment is set up due to the need to properly measure the change in voltage, as for areas of small increment saw large changes in voltages. Which insures a more detailed mapping of how the voltage is changing in such areas of more sudden voltage differences.

From the measured data, both voltage against frequency and current against frequency graphs would be presented. With resonance frequency identified as the global extremum within the set range.

4.4 Results

4.4.1 Data and Analysis

From the retrieved data, the following data (with uncertainties on the graph) presents Voltage measured across the resistor, $U_{P,R}$ and the Reduced Voltage $\frac{U_{P,R}(f)}{U_{P,R}(f_0)}$ against the varying Frequency input, f_P .

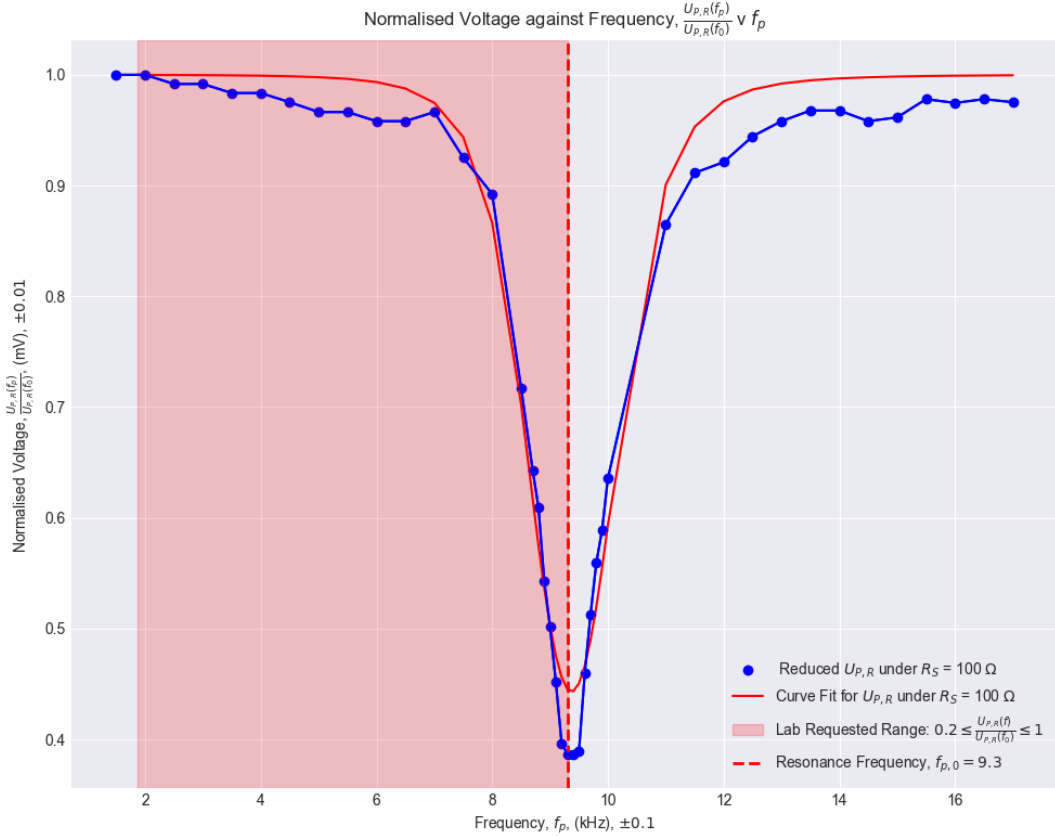


Figure 3: The Normalised Voltage against Frequency, $U_{P,R} \propto f_P$, with the region $\frac{U_{P,R}(f)}{U_{P,R}(f_0)}$ highlighted

Figure 3 presents the voltage change under a parallel configuration. As proposed in the hypothesis, section 4.1, the parallel configuration in this experiment highlights a band-stop filter. Where a drop, rather than a spike, is expected at and around the Resonance Frequency and a plateauing behaviour on both ends. Such hypothesis is confirmed with the above graph, where the resonance frequency was found to be **9.3 kHz**, highlighted in red - as the minimum value (correlating to the lowest point in the 'dip'). Which is within a $|-8.04597701149\%| \approx \mathbf{8.05\%}$ percentage error relative to $f_{S,0}$ from section 3. Further reaffirming the understanding that, for relevant enough resistance, that the resonance is dependent on the configuration of energy exchange and the strain under the resistor, rather than the set up of the circuit. In correlation to the model fit, seen in red, the theoretical data set corresponded to a R^2 score of $0.978879280544537 \approx \mathbf{0.979}$. Both the measured and theoretical curve fit data sets presented the similar trend of a sudden drop in approaching $f_o \propto P$. With an average difference of $4.199806602021055\% \approx \mathbf{4.20\%}$ between the theoretical and measured, and a Mean Absolute Error (MAE) of

$|0.016118817103119295| \approx \mathbf{0.02}$ and a Max Difference (MD) of $0.061150941336227616 \approx \mathbf{0.61}$, the Mode Curve Fit Data set is within a reasonable close approximation to the Measured Data Set. Allowing as to approximate the values of the R_d , L , R_{Sp} , and the C from the curve fit. These values came out to as follows:

Parameter	Curve Fit Value
$R_d (\Omega)$	≈ 95.46
$L (H)$	≈ -0.097
$R_{Sp} (\Omega)$	$\approx -1.145^*$
$C (s)$	≈ 0.003

Table 2: Found value from the curve fit for the parallel configuration

In the same retrospective, the following graph presents the above measurements but in terms of calculated Current. As such (with uncertainties on the graph) the calculated Current across the resistor, $I_{P,R}$ and the Reduced Current $\frac{U_{P,R}(f)}{U_{P,R}(f_0)}$ against the varying Frequency input, f_P is:

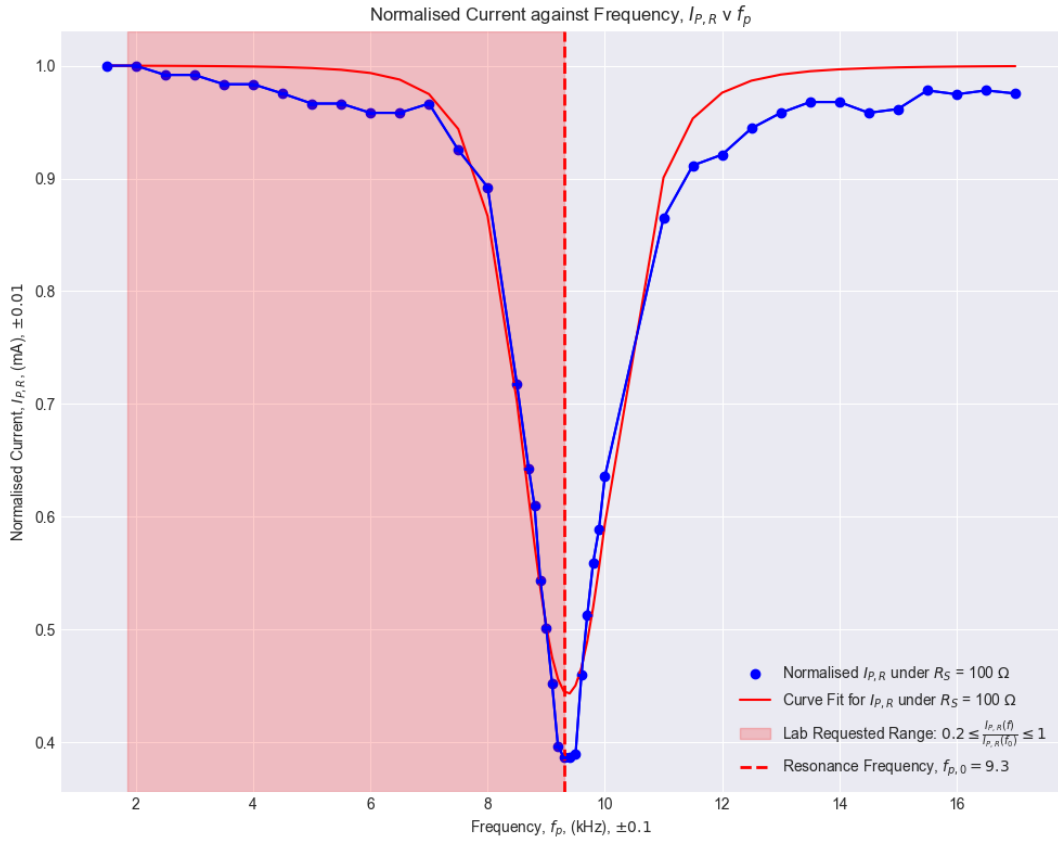


Figure 4: The Normalised Current against Frequency, $U_{P,R} v f_P$, with the region $\frac{U_{P,R}(f)}{U_{P,R}(f_0)}$ highlighted

In the same manner as discussed above, the behaviour is as expected. The Current's calculated and theoretical data sets came out to values (same as before as they vary

with only a constant R_2 and under normalised conditions it would have no effect) a R^2 score of $0.978879280544537 \approx \mathbf{0.979}$. Both the measured and theoretical curve fit data sets presented the similar trend of a sudden drop in approaching $f_{P,R}$. With an average difference of $4.199806602021055\% \approx \mathbf{4.20\%}$ between the theoretical and measured, and a Mean Absolute Error (MAE) of $|0.016118817103119295| \approx \mathbf{0.02}$ and a Max Difference (MD) of $0.061150941336227616 \approx \mathbf{0.61}$. Any further data analysis are omitted as they follow the results from the voltage measurements.

*The inconsistency with negative R_{sd} value, and further analysis of the results will be discussed in the Discussion below.

4.4.2 Discussion

From the above mentioned behaviour of the parallel set up of the RLC circuit, there is a clear expected behaviour with resultant values within the expected range. The negative element of R_{sd} is theoretically a physically possible answer (as negative resistance "exists") however it is a special case of circuits with the purpose of decreasing current with an increasing voltage. Proposing, bounding and setting standard expected guesses within the curve fit code did not lead to a more reasonable answer - where either the curve fit reached its max computational power or provided a curve with an R^2 value in the negatives. The derived final equation from section 4.2 equation 15, had been derived in consistency as seen for other circuit configurations, and as such any issues relating to the equation may be considered as negligible (as far as we are aware).

However, in the same retrospective, the magnitude of R_{sd} seems to be consistent with the expected values for a resistance of coil of the size provided for the experiment. Researching the exact make of the coil, and comparing the manufacture issued internal resistance, the value of $|-1.145| = 1.145$ seems within the range of expected value. The manufacture issued resistances, for the length of the provided inductor, ranged with a 0.3Ω increase for every 0.5 mH , from which 1.5 mH would correlate to about 0.9Ω . A percentage difference of $26.6666666667 \approx 26.7\%$. A relatively high number, but in the scale of $\approx 0.2 \Omega$ difference between resistance, seems to be a reasonable closely related values. A slight ramification of sign inconsistency to the validity of our data and results will be discussed near the end of this section, and how the values further discussed for other components below are to be taken under R_{sd} inconsistency.

In further understanding, the value of the R came out closely to what was expected, as the utilised resistor was 100Ω , with resultant value at a percentage difference coming out to $\approx 4.54 \%$ in relation to 95.46Ω . In the same manner, the values for Inductance and Capacitor relative to their respective values for the Series 100Ω RLC circuit, came out to a magnitude difference of $|0.147566566001| \approx \mathbf{0.148 \text{ H}}$ and $|-0.00157681202651| \approx \mathbf{0.001 \text{ F}}$ respectively. But with percentage difference of $60.2426100042 \approx \mathbf{60 \%}$ and $|-115.288239398| \approx \mathbf{115 \%}$ respectively. However, as the values of these values are within the same magnitude with a rounding difference of each other, they provide a reasonable understanding that the found capacitance and inductance are of the actual nature of the components used in the circuit.

As mentioned before, the resonance frequency, f_{oP} came out to 9.3 kHz , and the 8.05% difference in comparison to the series counterpart of the same resistor is of reasonable error margin. As an error difference of under 10% to the expected values can be approximated

to be difference due to non perfect system rather then issues from the experiment itself.

In the same manner as done for the series, the FWHM, Q factor and the 'damping' constant δ is to be found. Utilising the already explained method from section 3, the values came out to:

Parameter	Value
$FWHM$	15.5
Q factor	≈ 0.62
δ	≈ 48.70

Table 3: Found values; the FWHM, Q factor and δ utilising the curve fit.

Further research in this circuit will be understanding how different resistors, and different band-stop configurations affect the resonance frequency, the shape and the value of the resistances. To improve this experiment, procession of more data points, utilising a high resistor to increase the width of the dip, and attempting multiple trials would provide a more reasonable result set. If the above values are consistent throughout these changes (relative to their change), it would better reaffirm the final values.

The issue of validity of our data, being pointed out due to a sign inconsistency in one of the vital components of the circuit, comes into question. There is a very likely chance that the experiment, or the equation utilised to derive the curve fit, was wrong or incorrect to some extent. And the closeness of the other parameters with their series counterpart could be an unforeseen coincidence. It is one thing to be off by a large margin, yet to get a result which is technically impossible in the context of our experiment (the negativity) is a gaping problem. Even though thorough research and check of our understanding and approach, the calibration of the circuits, control of the input voltage and derivation of the formula were done, there is clearly an issue somewhere. It is important to acknowledge how the above data has to be taken through a more attentive attention.

4.4.3 Error Analysis

The uncertainty, as also seen on each graph for respective uncertainty, for the measured voltage data set is the smallest measurable value on the provided software. While the uncertainty for the Model Curve Fit Data Set is calculated following the equations of John R. Taylor, from An Introduction to Error Analysis: The Study of Uncertainties in Physical Measurements (Taylor):

$$\sigma_{U_{P,R}} = \left| \frac{\partial U_{P,R}}{\partial \omega} \right| \cdot \sigma_{\omega} \quad (16)$$

where utilising the above equation gives,

$$\sigma_{U_{P,R}} = \left| \frac{-U_0 R \cdot x(\omega)}{(R^2 + x(\omega)^2)^{3/2}} \cdot \frac{dx}{d\omega} \right| \cdot \sigma_{\omega} \quad (17)$$

and when propagating the uncertainty through equation 17, leads to the summary of the uncertainties for the parallel circuit as:

Data Set	Mean Error Propagation	Largest Error (Max)
Model Curve Fit Voltage	$\pm 3.72 \cdot 10^{-10}$	$\pm 3.28 \cdot 10^{-9}$
Measured Voltage	± 0.01	± 0.01

Table 4: Error Propagation; Mean and Maximum Values

5 Conclusion

The exploration of RLC resonant circuits has confirmed the theoretical predictions regarding resonance behavior in both series and parallel configurations. For the series circuit, a clear band-pass characteristic was observed, while the parallel configuration demonstrated the expected band-stop behavior. Despite variations in resistance, resonance frequency remained largely consistent, validating the independence of from resistance under ideal conditions. Experimental measurements using PicoScope, complemented by curve fitting and FWHM analysis, allowed for precise estimation of circuit parameters, including δ and the Q factor. While curve fitting proved more effective for broader resonant peaks, FWHM offered robustness in analyzing sharper, more sensitive configurations. Minor discrepancies, such as unexpected shifts in capacitance or negative component values, highlighted the challenges in practical circuit modeling and measurement. Nonetheless, the experiment successfully demonstrated the core dynamics of resonant circuits and emphasized the importance of careful analysis in both educational and applied electronics contexts.

6 Citation

Ziese, M. *E12He RLC Resonant Circuits*. Universitat Leipzig, Apr. 2025.

Ziese, M. *Practical Physics*. Universitat Leipzig, Apr. 2025, pp. 50–53.

PicoScope 2000 Series. Pico Technology,
<https://www.picotech.com/download/datasheets/picoscope-2000-series-data-sheet.pdf>.
Accessed 22 Apr. 2025.

Calculator.net. *Resistor Calculator*.
<https://www.calculator.net/resistor-calculator.html?bandnum=4&band1=brown&band2=brown>.
Accessed 22 Apr. 2025.

Wikipedia contributors. *RLC Circuit à Series RLC Circuit*. Wikipedia,
https://en.wikipedia.org/wiki/RLC_circuit#Series_RLC_circuit. Accessed 22
Apr. 2025.